Supplementary Information

Hard materials from Sulfur vulcanization of biochar

Chaza Al Akoumy[1], Mohamed Amin Mezour[2], and Richard Martel[1]*

[1] *Department of Chemistry and Institut Courtois, University of Montreal, Montreal, Quebec H3C 3J7, Canada.* [2] *Elkem Biocarbon, Chicoutimi, Canada*

* *r.martel@umontreal.ca*

1) Characterization of biochar

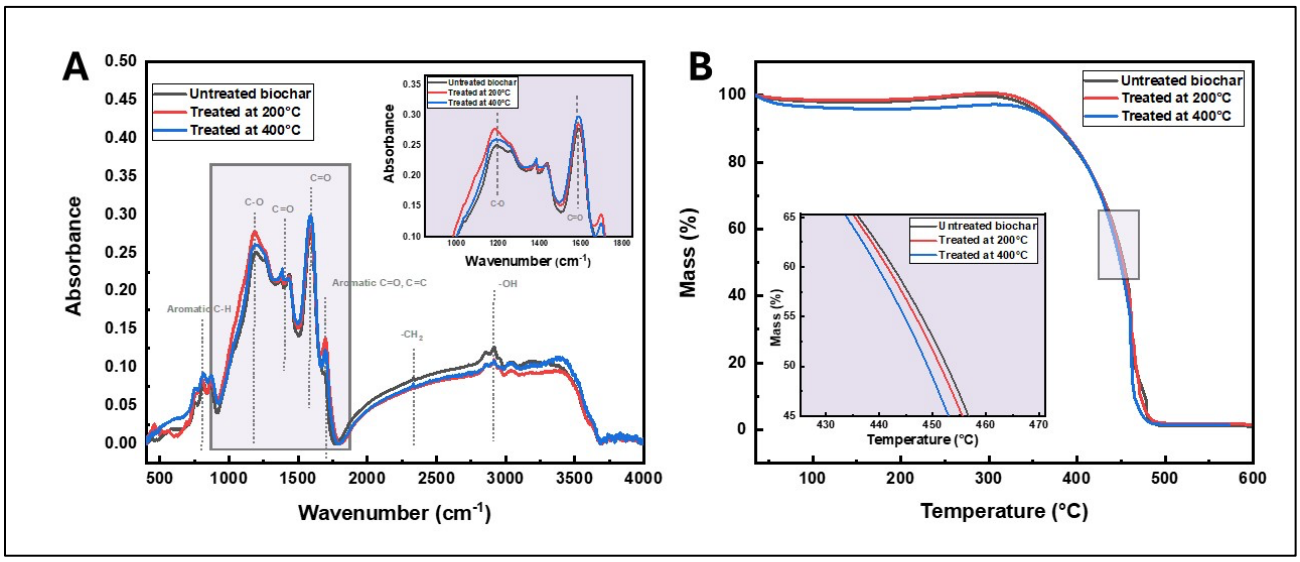

Figure S1 : Characterization of biochar reactivity: **(A)** FTIR spectra showing absorbance bands corresponding to biochar for untreated biochar, biochar treated at 200°C and biochar treated at 400°C, while highlighting the increase in absorbance of oxygenated groups with increasing of temperature, **(B)** TGA spectra of untreated biochar, biochar treated at 200°C and biochar treated at 400°C showing the increase of biochar reactivity with temperature by decreasing its degradation temperature with increasing thermal treatment temperature.

Table S1: Biochar characteristics: density and elemental analysis*

Biochar density (g/cm^3)	Elemental analysis			
	%N	%C	%H	%S
0.6	-	76.52 ± 0.07	3.55 ± 0.01	-

* Oxygen content cannot be measured by elemental analysis, but a value of about 20% in oxygen content can be estimated in biochar, assuming the residual element is only composed of oxygen.

2) Experimental Setup

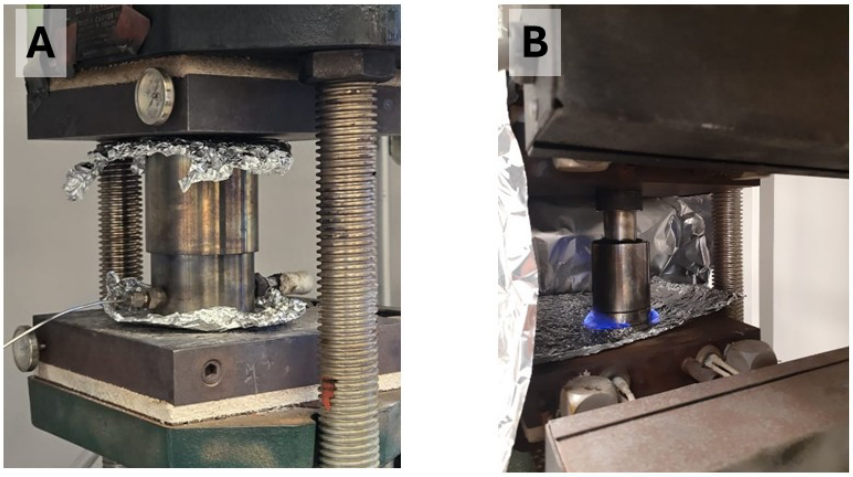

Figure S2: A) Photo of the experimental reactor under nitrogen, showing two cylinders with a gas inlet and a thermocouple inlet. B**)** photo of the mold being heated and pressed, with biochar and sulfur inside. A blue flame (SO_2) appears during heating under air.

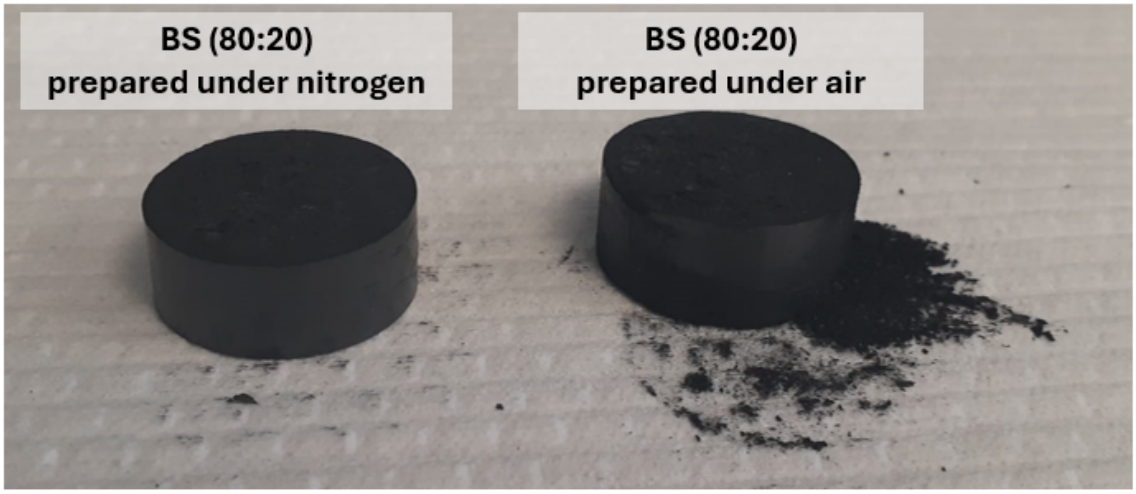

Figure S3: Photo showing the appearance of BS(80:20) prepared under different atmospheric conditions: air and nitrogen. The pellet prepared under air, without enough sulfur, is brittle. The BS(80:20) pellet prepared under nitrogen is hard and solid.

3) Porosimetry and Elemental Analysis

Table S2: Mercury intrusion porosimeter (MIP) results for biochar, BS(60:40) and BS(20:80) pellets after the first and second pressure steps, under nitrogen.

Sample	Total pore area (m^2/g)	Average pore diameter (µm)	Minimum pore diameter (µm)	Maximum pore diameter (µm)	Porosity (%)	Total pore volume (mL/g)	Skeletal apparent density (g/mL)
Biochar	3.524	2.35	0.6	32.9	67.0	2.071	1.00
BS(60:40) First pressure step	0.468	1.39	4.0	18.1	18.0	0.163	1.35
BS(20:80) First pressure step	0.766	0.57	8.0	15.4	12.4	0.109	1.28
BS(60:40) Second pressure step	1.756	0.61	4.0	17.3	13.8	0.164	1.41
BS(20:80) Second pressure step	0.036	1.24	4.0	7.2	6.0	0.015	1.42

Table S3: Mass, height, density and elemental analysis of BS(60:40) and BS(20:80) obtained after only one pressure step at 150°C under nitrogen flow and after two pressure steps in air and under nitrogen.

Sample	Mass of Biochar added (g ± 0.01)	Mass of sulfur added (g ± 0.01)	Total mass before reaction (g ± 0.01)	Total mass after reaction (g ± 0.01)	Δm (g)	Pellet height (mm)	Pellet density (g/ml)	N atm %	C atm %	H atm %	S atm %
BS(60:40)	3.60	2.40	6.00	5.22	0.78	8.34 ± 0.07	1.19 ± 0.01	0.080 ± 0.003	42.510 ± 1.514	1.990 ± 0.063	45.450 ± 0.476
BS(20:80)	1.20	4.80	6.00	3.38	2.62	5.31 ± 0.04	1.38 ± 0.06	0.0500 ± 0.0001	28.110 ± 0.678	1.320 ± 0.018	64.380 ± 0.846

Table S4: Mass, height, density and elemental analysis (in atomic %) of BS(60:40) and BS(20:80) obtained before reaction and after reaction (two pressure steps) at 185°C in air and under nitrogen.

Sample BS **% Mass**	**Mass of Biochar** (**g** ± 0.01)	**Mass of Sulfur** (**g** ± 0.01)	**C initial** atm %	**S initial** atm %	**C after** atm %	**S after** atm %	**C/S ratio**	**H Analysis** atm % ± 0.1	**C/H ratio**
BS(60:40) in air	3.53	2.47	69.6	30.4	59.9±0.4	27.4± 0.6	2.2	2.5	28.6
BS(60:40) in nitrogen	3.60	2.40	70.6	29.4	59.0±1.4	25.4±1.5	2.3	2.7	25.9
BS(20:80) in air	1.22	4.82	28.8	71.2	50.3±1.1	39.1±1.5	1.3	2.1	24.0
BS(20:80) in nitrogen	1.20	4.80	28.6	71.4	56.3±0.7	29.0±0.9	1.9	2.6	20.6

Table S5: Summary of elemental analysis results (in mass % and atomic %) for BS pellets prepared under a nitrogen atmosphere at 185°C.

Sample BS %Mass (Biochar:Sulfur)	C analysis		S analysis	
	atomic %	mass%	atomic %	mass%
BS(80:20)	62.8 ± 0.4	46.10 ± 0.03	20.7 ± 0.2	40.42 ± 0.50
BS(60:40)	59.0 ± 1.4	41.24 ± 0.07	25.4 ± 1.5	47.38 ± 0.80
BS(40:60)	54.1 ± 0.6	35.36 ± 0.90	30.7 ± 0.6	53.57 ± 0.70
BS(20:80)	56.3 ± 0.7	37.51 ± 0.09	29.0 ± 0.9	51.54 ± 0.92

4) Morphological Analysis

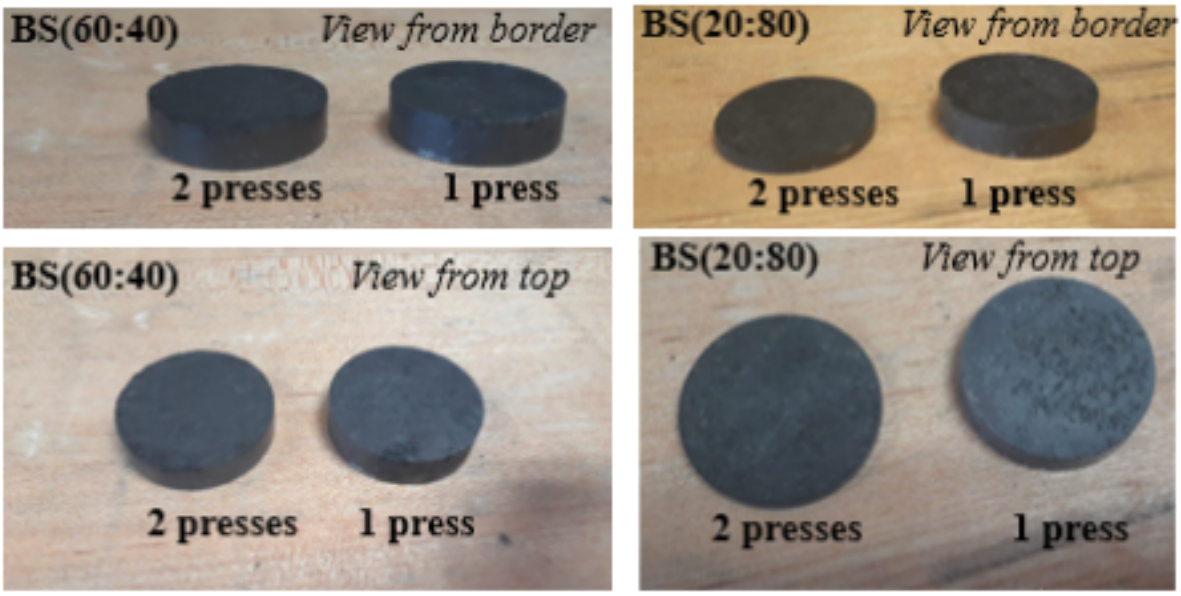

Figure S4: Optical micrographs of BS(60:40) and BS(20:80) pellets for surface appearance and height after the first and second pressure steps under nitrogen. The pellets obtained after the first pressure step at 150°C are more porous and thicker than the pellets obtained after the second pressure step at 200°C.

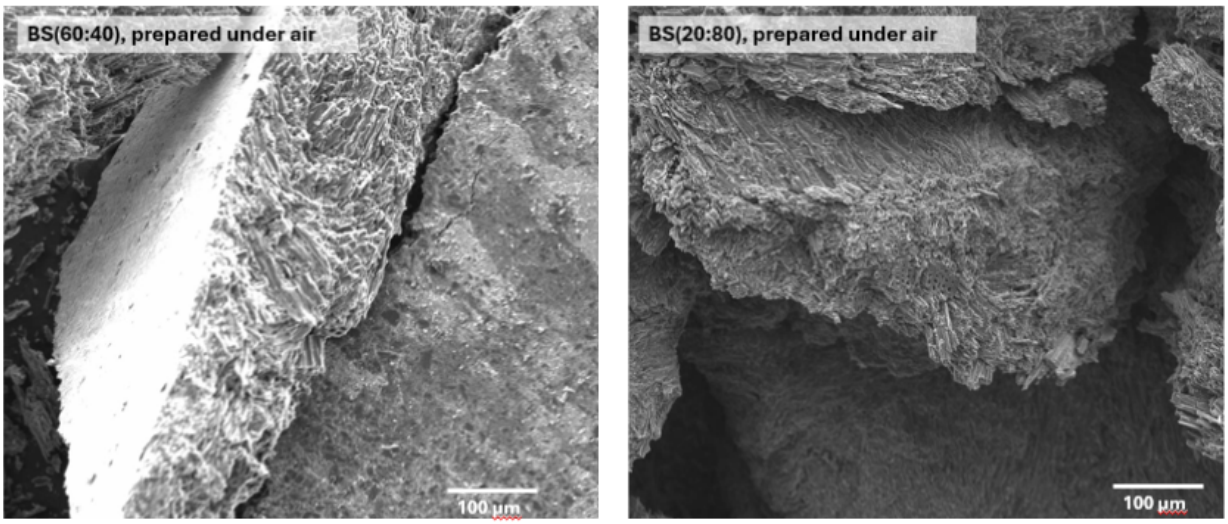

Figure S5: SEM images of BS(60:40) and BS(20:80) prepared in air.

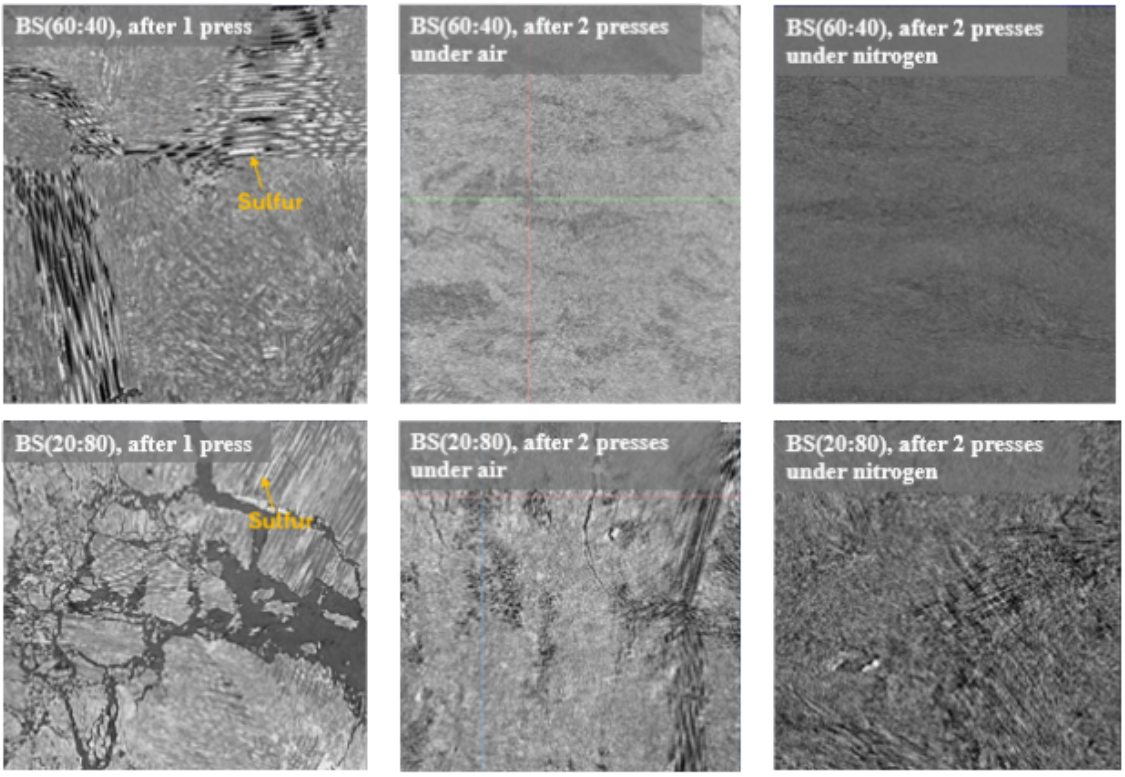

Figure S6: 3D X-ray tomography images for biochar-sulfur pellets BS(60:40) and BS(20:80) after the first and second pressure steps in air and under nitrogen.

Table S6: Porosity (%) obtained by processing of X-ray tomographic images of BS(60:40) and BS(20:80) after the first and second pressure steps in air and under nitrogen.

Sample	Total porosity (%)
BS(60:40), first pressure step	10.06 ± 0.59
BS(60:40), second pressure step under nitrogen	2.35 ± 0.35
BS(60:40), second pressure step under air	10.95 ± 0.43
BS(20:80), first pressure step	17.10 ± 0.71
BS(20:80), second pressure step under nitrogen	3.64 ± 0.97
BS(20:80), second pressure step under air	11.68 ± 0.62

5) FTIR and Raman of BS Materials

Due to the shape of a 2D band near 2500 cm^{-1}, the Raman spectra of BS(60:40) and BS(20:80) (**Figure S7A**) indicate after reaction that the carbonaceous backbone is mainly amorphous graphitic-like carbon. Two main peaks are present in the D-band (1300-1400 cm^{-1}) and G band (1550-1610 cm^{-1}) regions, which are also typical in graphitic materials and related to C-C sp^3 and C=C sp^2 stretching modes, respectively[S1,S2]. However, the C-S modes expected at 1050 cm^{-1} and thiophene-like C-S-C modes at 1450 cm^{-1} cannot be confirmed due to overlap with the broad D and G bands. The spectra present no evidence either of disulfide S-S modes at 480 cm^{-1}. Additional FTIR measurements (**Figure S7 B)** show, however, that these bands are indeed present at 470 cm^{-1} in both the BS(60:40) and BS(20:80) samples and absent in as-received biochar. C-S stretching bands at around 830-600 cm^{-1} and S-H bending vibrations at 2654-2521 cm^{-1} are either absent or masked by other strong bands related to C-H bending from aromatic rings (950-600 cm^{-1}) and other C-H stretching bands in biochar[S3].

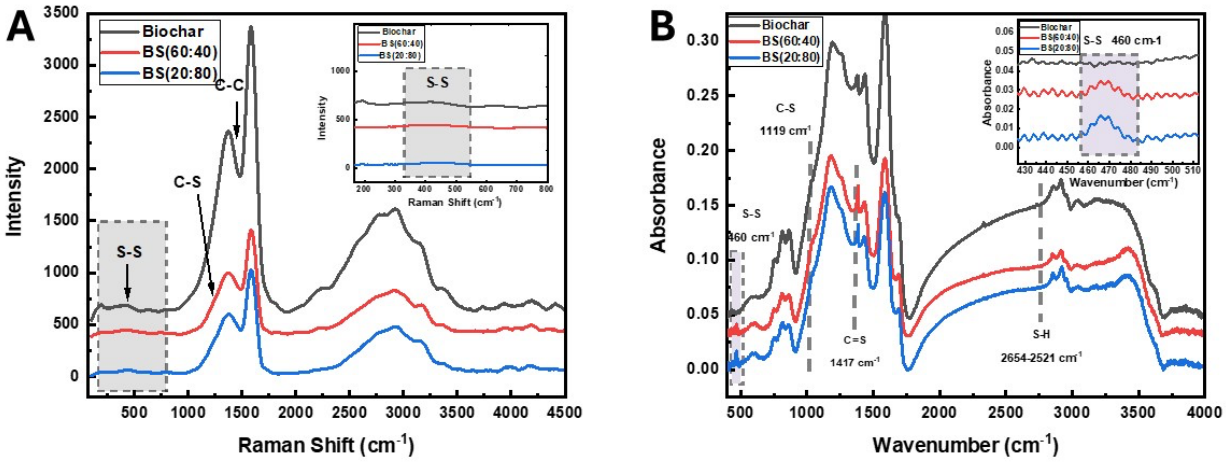

Figure S7: (A) Raman spectra and **(B)** FTIR spectra of biochar, BS(60:40) and BS(20:80) prepared under nitrogen.

6) Mechanical Testing

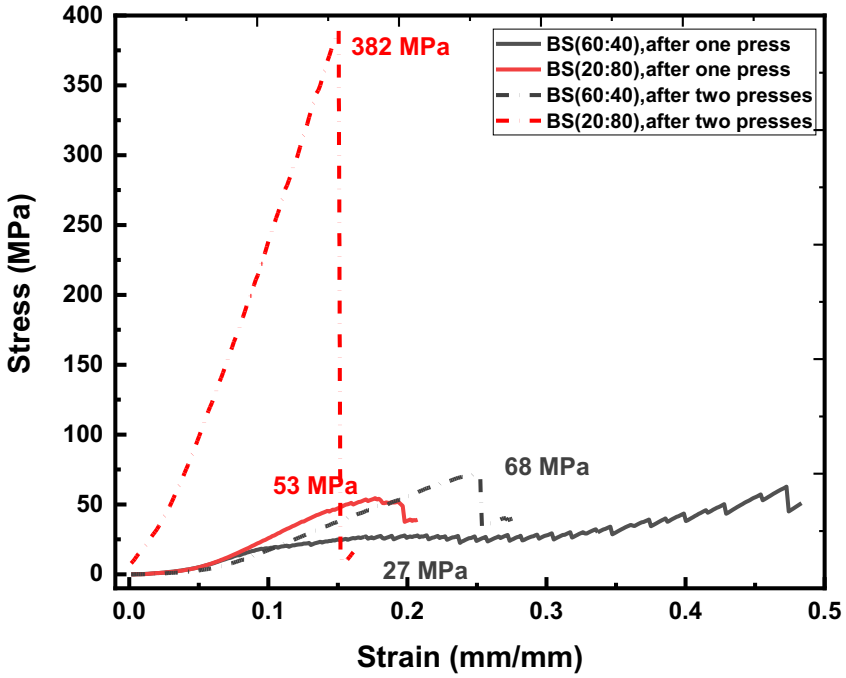

Figure S8: Stress-Strain curve by axial compression for BS(60:40) and BS(20:80) after the first and second pressure steps under nitrogen.

Table S7: Comparison of compressive strength between all the BS pellets prepared in air and under a nitrogen flow with that of commercial materials

Material	Compression breaking force (N)	Compressive strength (MPa)	Reference*
BS(80:20) prepared under air	11880 ± 1200	23± 2	this work
BS(60:40) prepared under air	23824 ± 3100	47 ± 6	this work
BS(40:60) prepared under air	45855 ± 3400	91 ± 7	this work
BS(80:20) prepared under air	48974 ± 4700	97 ± 9	this work
BS(80:20) prepared under nitrogen	14792 ± 2100	29 ± 4	this work
BS(60:40) prepared under nitrogen	34465 ± 3800	68 ± 8	this work
BS(40:60) prepared under nitrogen	42932 ± 6000	85 ± 8	this work
BS(20:80) prepared under nitrogen	193760 ± 3800	383 ± 8	this work
Structural (low carbon) steel AISI-SAE 1020	-	180**	37
Polyethylene terephthalate (PET)	-	80 (90-140)	S4, (35)
Polycarbonate (PC)	-	40 (80-105)	S4, (35)
Acrylonitrile butadiene-styrene (ABS)	-	70-80	39
Straw biochar briquettes with additives (sulfur and lignin) added as binders	-	1.5	45
Pellet biochar - lignin	-	22	38
Carbon fibers	-	2330	42
Concrete	-	17-30	40
Mortar (Portland Ciment)	-	49	12

***See references in the main text**

**** Yield strength value is used (yield strength = compressive strength for ductile materials)**

Table S8: Comparison of the Young modulus between different biochar-sulfur pellets prepared under air and nitrogen with other commercial steel and concrete materials

Type of material	Material	Young modulus (GPa)	Reference*
Biochar-sulfur pellets	BS(80:20) under air	6	_
	BS(60:40) under air	8	_
	BS(40:60) under air	12	_
	BS(20:80) under air	12	_
	BS(80:20) under N_2	5	_
	BS(60:40) under N_2	21	_
	BS(40:60) under N_2	95	_
	BS(20:80) under N_2	165	_
Steel	Carbon steel	210	S5
	stainless steel (405)	200	S5
Carbon Fiber	PAN precursor	230-400	S5
Plastics	PET	2.76-4.14	S5
	Nylon 6,6	1.59-3.79	
	Polycarbonate	2.4	
Concrete	Normal Weight Concrete	28-41	S6, 43
	Lightweight Concrete	14-28	
	High-Strength Concrete	34-48	
	Fiber-Reinforced Concrete	28-41	
	Prestressed Concrete	41-55	

- **See references in the main text**

7) Thermal Properties

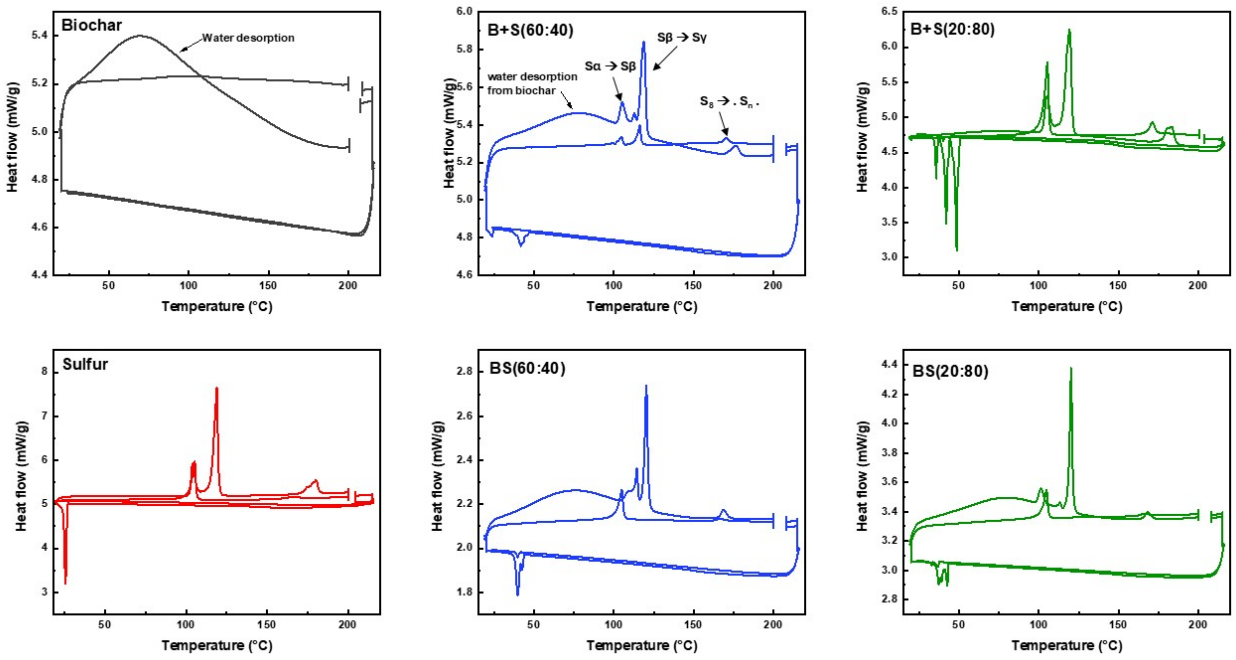

Figure S9: DSC curves under a nitrogen flow are shown for biochar (black) and elemental sulfur (red) and compared with B+S(60:40) and BS(60:40) samples containing 40% sulfur (blue), as well as B+S(20:80) and BS(20:80) samples containing 80% sulfur (green). Here, B+S refers to a mixture of biochar and sulfur placed directly into the crucible, with the reaction occurring during the DSC measurements. BS refers to reacted samples obtained by grinding BS pellets after reaction.

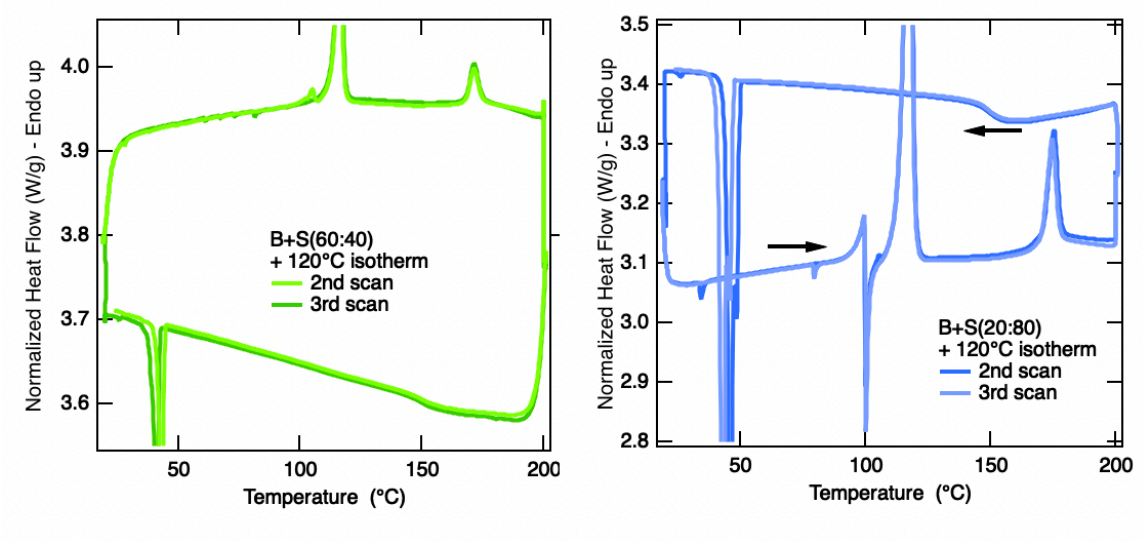

Figure S10: DSC curves under a nitrogen flow of B+S(60:40) and BS(60:40) samples containing 40% sulfur (green) and 80% sulfur (blue) following a 90 min isothermal step at 120°C during the

first scan only. Here, B+S refers to a mixture of unreacted biochar and sulfur placed directly into the crucible with the reaction occurring during the DSC measurement.

Corrections Factor for the Sulfur Content

DSC were performed on different mixtures of biochar and elemental sulfur, and they were also acquired on pellets after reaction. Initially, the enthalpies of each transition were measured by integration of the peak and the value was then normalized per gram of materials.

To convert this enthalpy value from J/(g of sample) to J/(g of sulfur), we have divided the experimental enthalpy value by the sulfur content in gram. As an important note, this estimate only provides the sulfur content of crystalline forms of sulfur. There may be additional sulfur present in an amorphous state.

As an example, B+S(60:40) provides a enthalpy value of 16.13 J/g. The sulfur content to prepare the mixture was 40% in mass of sulfur, which is 0.4 g sulfur per 1 g of B+S sample. Therefore, the enthalpy measured in J/(g of sulfur) is 16.13 *0.4 J/g = 6.45 Joules per gram of sulfur.

The special case of BS(60:40) and BS(20:80) requires an additional correction because the atomic percentages of sulfur in these samples were determined after reaction by elemental analysis (see Table S8 below). To make this correction, we have first calculated the mass ratio of carbon and sulfur for each sample using the formula:

$$M\%\,ratio(C) = \frac{C(atomic\%)*Mc}{(C(atomic\%)*Mc)+(H(atomic\%)*MH)+(N(atomic\%)*MN)+(S(atomic\%)*MS)+(O(atomic\%)*MO)} * 100,$$

where C(atomic)% is the atomic composition and Mc, Mo, M_H, M_N, and M_S correspond to the molar masses of our C, O, H, N and S. Using the same formula, we obtained the M% (S) of sulfur:

$$M\%(S) = \frac{S(atomic\%)*MS}{(C(atomic\%)*Mc)+(H(atomic\%)*MH)+(N(atomic\%)*MN)+(S(atomic\%)*MS)+(O(atomic\%)*MO)} * 100$$

As an example, the elemental analysis results are of BS(60:40) is:

Atomic% of N: 0.09 ± 0.01

Atomic % of C: 59.00 ± 1.36

Atomic % of S: 25.39 ± 1.48

Atomic % of H: 2.73 ± 0.08

Because oxygen cannot be probed by the analysis, we can safely assume that the rest corresponds to the oxygen atomic %, giving 12.80. We calculated the M% ratio (C) using:

$$\text{M\% ratio (C)} = \frac{59*12.011}{(59*12.011)+(2.73*1.008)+(0.09*14.007)+(25.39*32.065)+(12.08*15.99)} = 0.4124$$

Then M%(C) is : 41.24%.

In the same way, the M% ratio (S) is given by:

$$\frac{25.39*32.065}{(59*12.011)+(2.73*1.008)+(0.09*14.007)+(25.39*32.065)+(12.08*15.99)} = 0.4738$$

, which can be used to give M%(S) of 47.38%.

Table S9: Enthalpies, ΔH, for each phase transitions of S, B+S (60:40), B+S (20:80), BS (60:40), and BS (20:80) samples using DSC measurements performed using two heating cycles (20°C – 200°C, 10°C/min), along with their corresponding sulfur atomic percentages from recipe or elemental analysis (after reaction).

Sample		1st heating cycle			2nd heating cycle			Content of S (atomic %)
		S_α to S_β	$S_{melting}$	S to poly-S	S_α to S_β	$S_{melting}$	S to poly-S	
S	ΔH (J/g)	11.7	44.1	10.0	16.7	-	0.7	100
	ΔH*(J/g of S)	11.7	44.1	10.0	16.7	-	0.7	
	temperature (°C)	104.1	118.8	178.1	104.7	-	165.5	
B+S(60:40)	ΔH (J/g)	3.3	12.0	3.05	7.2	-	1.7	22
	ΔH*(J/g of S)	6.9	30.1	6.48	15.3	-	3.6	
	temperature (°C)	118.4		176.5	116.2	-	170.7	
BS(60:40)	ΔH (J/g)	3.7	9.3	1.03	3.0	1.02	0.2	25.4±1.5
	ΔH*(J/g of S)	7.8	19.8	2.19	6.3	2.17	0.4	
	temperature (°C)	114.2	119.8	167.5	109.4	115.5	167.6	
B+S(20:80)	ΔH (J/g)	12.2	45.1	12.8	0.4	-	9.1	63
	ΔH*(J/g of S)	15.2	56.4	16.0	0.4	-	11.4	
	temperature (°C)	103.8	119.5	167.5	109.4	115.5	167.6	
BS(20:80)	ΔH (J/g)	2.1	12.0	1.3	3.9	-	0.8	29.0±0.9
	ΔH*(J/g of S)	4.0	23.5	2.5	7.6	-	1.6	
	temperature (°C)	101.2	120.1	168.1	104.6	-	166.9	

*The ΔH has also normalized using the content of sulfur and is also given in units of joule per gram of sulfur in each sample.

Calculation of the percentage of residual S_8 in the BS samples, $\Delta\chi\%$, with respect to elemental sulfur is given by:

$$\Delta\chi\,\% = \left[\frac{\Delta H_m}{\Delta \mathrm{H}_m(\mathrm{S})}\right] \times 100\,\%$$

, where ΔH_m is the melting enthalpy of sulfur in BS sample and $\Delta \mathrm{H}_m(\mathrm{S})$ is the melting enthalpy of elemental sulfur. The values used and from Table S8, first scan ΔH_m values of the experimental DSC experiments.

Table S10: Percentage of residual crystalline S_8 in BS samples: B+S (60:40), B+S (20:80), BS (60:40), and BS (20:80), obtained from the first DSC scans.

	Fraction, Δχ%	Melting Temperature, T_m °C
S	100	119
B+S(60:40)	68*	118
BS(60:40)	45	120
B+S(20:80)	127*	119
BS(20:80)	53	120

- Note that the difference in mass when compared to the targeted masses for B+S samples is likely due to a non-uniformity in the mass distribution during the sample preparation for DSC measurements.

8) XRD Results

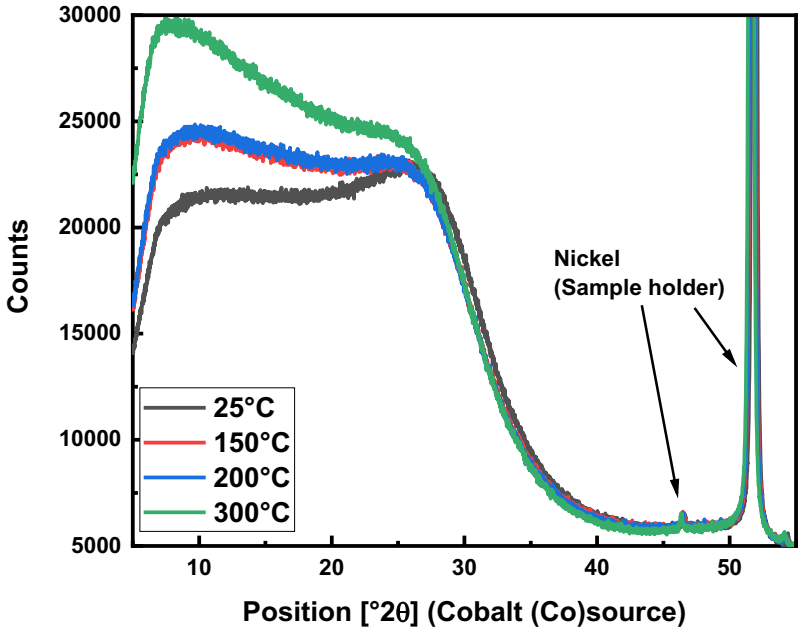

Figure S11: Biochar X-ray diffraction (XRD) measured at different temperatures: 25°C (black); 150 °C (red); 200 °C (blue); and 300 °C(green). Data acquired using the unfiltered cobalt radiation source at λ = 1.79 Å. As a note, the diffraction peaks are from the nickel sample holder and the broad signal, which shifts toward lower angles with temperature, is due to thermal expansion.

9) Tests for toxic gas (H_2S and SO_2) during synthesis

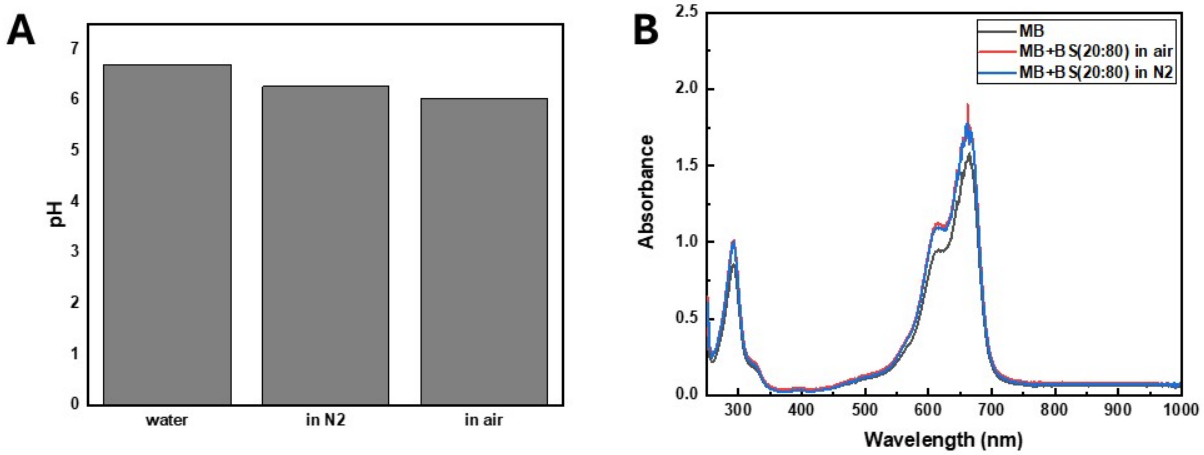

Figure S12: (A) pH measurements of deionized water before and after bubbling the gas produced during the synthesis of BS(20:80) under air and nitrogen atmospheres. (B) UV-Vis spectra of methylene blue (MB) before and after exposure to test possible H_2S gas produced during the synthesis of BS(20:80) under air and nitrogen atmospheres. No red-shifted peak is detected indicating no significant production of H_2S.

10) TGA Results

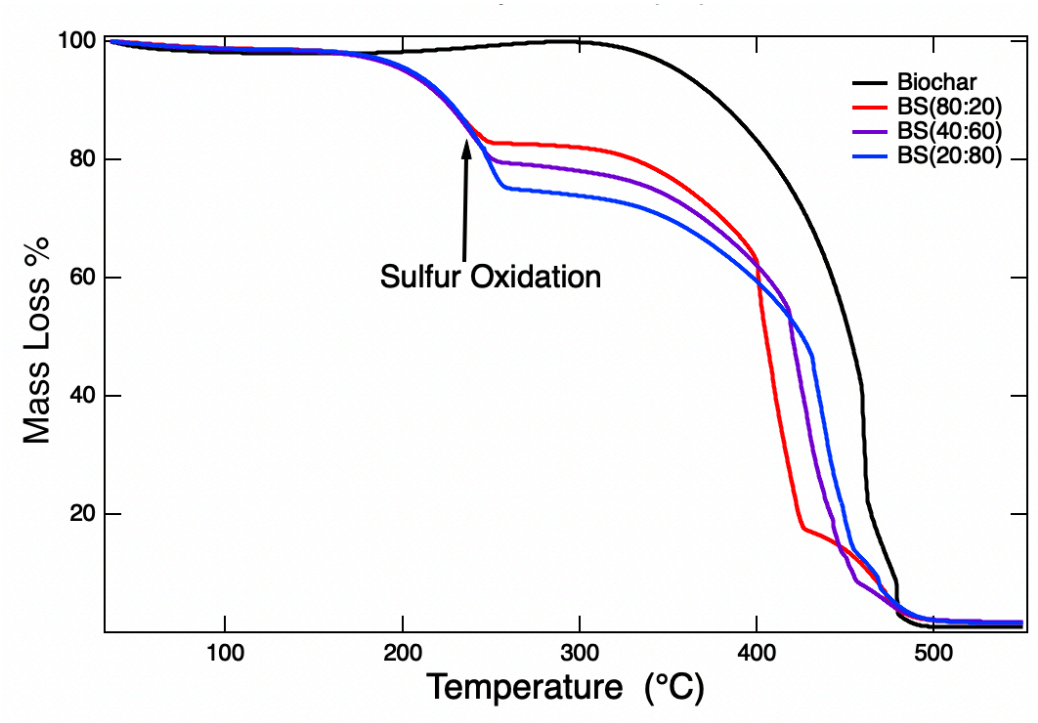

Figure S13: TGA curves of biochar and of different BS pellets prepared with different sulfur contents.

11) Electron Paramagnetic Resonance

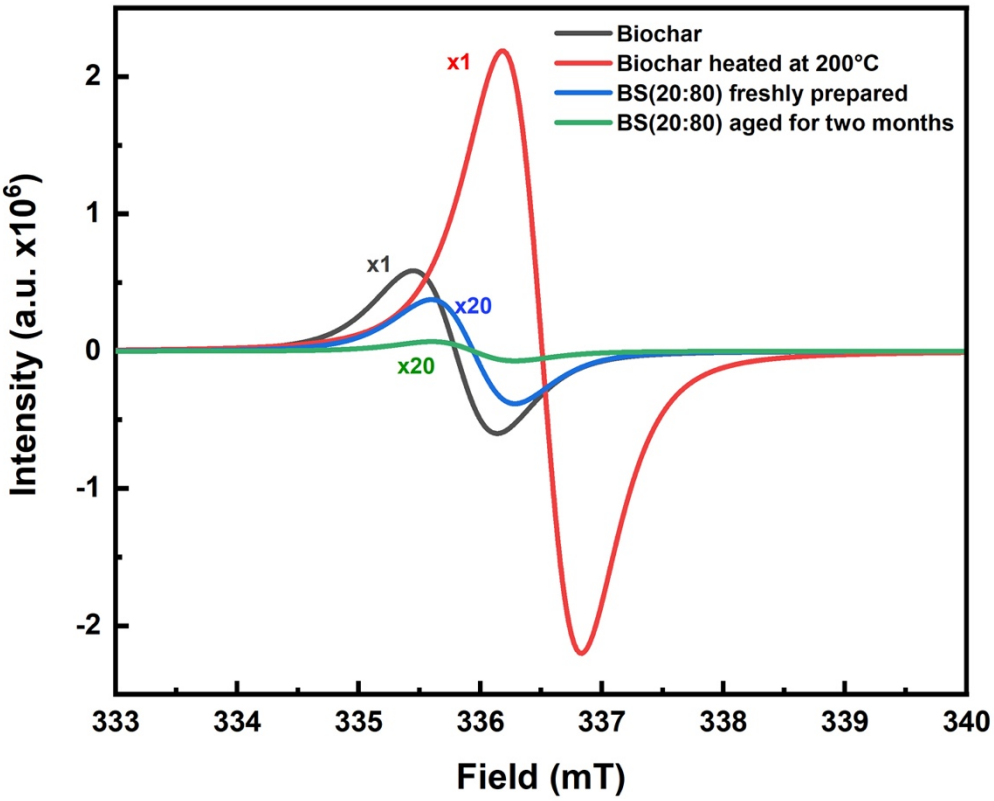

Figure S14: Electron Paramagnetic Resonance (EPR) spectrum of biochar (black) and activated biochar in air at 200°C (red) compared to that of a BS(20:80) sample freshly prepared under nitrogen atmosphere (blue) and that of the same sample aged for 2 months in air (green).

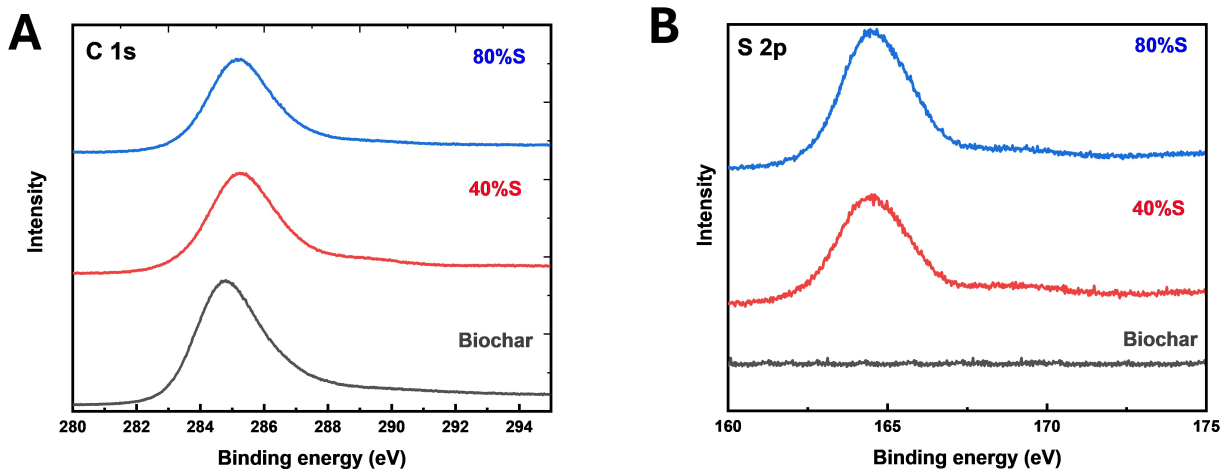

Figure S15: Raw XPS spectra of the **(A)** C 1s and **(B)** S 2p regions of biochar, BS(60:40) and BS(20:80).

References

S1. Robertson, J. Diamond-like amorphous carbon. *Mater. Sci. Eng.* **37**, 129–281 (2002).

S2. Matta, S., Bartoli, M. & Frache, A. Investigation of Different Types of Biochar on the Thermal Stability and Fire Retardance of Ethylene-Vinyl Acetate Copolymers. *Polymers (Basel).* **13**, 1256 (2021).

S3. Zhang, H. *et al.* Enhanced mercury removal by transplanting sulfur-containing functional groups to biochar through plasma. *Fuel* **253**, 703–712 (2019).

S4. Mittal, A. Compressive Strength Of Plastics The Ultimate Guide. PlasticRanger (2023).

S5. *Callister.W.D, JR. Materials Science and Engineering: An Introduction. 7th edition. (John Wiley & Sons, Inc., 2007).*

S6. Mehta, P. & J.M. Monteiro *Concrete: microstructure, properties and materials*. (McGraw-Hill Education, 2006).